

## Numerical Study of Permanent Deformations of Embankment dams under Seismic Loading, A case study of Kheyraabad Dam

Masoud Oulapour <sup>\*1</sup>  
Mohammad Amjadzadeh <sup>1</sup>  
Hossein Samani <sup>1</sup>

### Abstract

Considering the developments of new accurate constitutive models and numerical methods, a comparison between the classical and modern numerical methods of dynamic analysis of earthfill dams seems necessary. A three steps procedure was followed in this study. First, the accelerations and displacements of a typical homogenous dam were calculated using Sarma, Makdisi-Seed, and Sarma-Ambraseys methods, the results were compared with the results of Quake/W and Slope/W software using both linear elastic and equivalent linear models. Then, a special code was developed to calculate the deformations of a given wedge of the dam body based on the outputs of numerical analyses and the Newmark double integration method. The studies showed that due to the use of linear elastic behavior model, which is different from the real soil behavior, the critical acceleration estimated in classic methods is different from the reality and leads to oversized design. However, the more realistic constitutive models give better results. Also, in classic methods the shape of the wedges was unrealistic as it was assumed to pass through the core of the dam, while in numerical analysis it was shown that the critical wedge passes through downstream shell. Therefore, since the shape of critical wedges in homogeneous dams was completely different from the assumed shape of critical wedges in classic methods, the critical acceleration of wedges was different from the predictions of the classic models, for example it was estimated to be 0.41g in the Ambraseys-Sarma method compared to 0.31g in the linear method for a wedge depth of 60% of dam height. It was concluded that numerical methods with more realistic constitutive models must be used. Finally, the Kheyraabad embankment dam was analysed using the developed method. It was concluded that the dam would show a permanent deformation of 0.04 m under scaled Naghan earthquake.

**Keywords:** Embankment dams, Dynamic analysis, Critical Acceleration, Permanent Deformations, Equivalent Linear model.

Received: 07 August 2024; Accepted: 24 September 2024

\* E-mail: [Oulapour\\_m@scu.ac.ir](mailto:Oulapour_m@scu.ac.ir) (Corresponding Author)

<sup>1</sup> Department of Civil Engineering, Faculty of Civil Engineering and Architecture, Shahid Chamran University of Ahvaz, Ahvaz, Iran.



## 1. Introduction

Earth dams are massive three-dimensional and non-homogeneous structures composed of multi-phase, non-linear elastic materials. Therefore, their dynamic analysis under earthquake loading is one of the most complex problems in dam engineering. Recent advances in computer hardware and software, as well as the growing development of numerical methods for solving engineering problems, have overcome the problems related to these complexities, especially in the nonlinear behavior of dam materials. The early studies on the seismic stability of earth dam slopes can be attributed to the research of Mononobe et al. [1]. They initially proposed the shear beam method, which did not gain much attention due to the extensive computations required. In this method, the dam structure is assumed to be deformable, and its cross-section is divided into very thin horizontal layers, connected by linear elastic shear springs and viscous dampers. Later, Terzaghi [2] proposed the pseudo-static method and these methods were widely used then and are still somewhat relevant today. The basic assumption in the Terzaghi method was that the dam body behaves as a rigid body. Therefore, the effective acceleration in all its sections and at any height is equal to the maximum ground acceleration. Newmark [3] introduced the sliding block method, which is still in use by engineers and researchers due to its simplicity and practicality. Permanent deformations can be calculated for any specified sliding wedge using this method. Goodman and Seed [4] showed that the Newmark model gives acceptable results for highly cohesive soils. Seed [5] showed that an accurate determination of critical acceleration is very crucial for the estimation of permanent displacement. The development of the finite element method and its application in dynamic slope stability analysis led to a significant advancement in dam analysis methods. Ambraseys and Sarma [6] studied the response of earth dams under a group of important earthquakes and calculated the time history and distribution of acceleration in the dam body. Sarma [7] developed charts for calculating critical horizontal acceleration, where the critical horizontal acceleration is defined as the acceleration which can take the soil mass of the sliding wedge to a limit equilibrium state. Sarma [8] investigated the sensitivity of calculating permanent displacements to the parameters used in determining critical acceleration, such as dimensional coefficients and wedge geometry. Sarma [9] used the Newmark analysis model to show the effects of inertial forces and pore water pressure on the safety factor, critical acceleration, and displacements of potential sliding surfaces. This analysis was based on the principles of limit equilibrium, and the materials followed the Mohr-Coulomb failure criterion. Soil resistance parameters were also based on effective stress parameters. Makdisi and Seed [10] analyzed several different dams using the QUAD-4 program and calculated permanent deformations on assumed sliding surfaces using the Newmark sliding block method based on the movement of the block on the inclined surface. Seed [11] stated that if a dam is designed with a pseudo-static earthquake coefficient between 0.1 and 0.15 and a safety factor of 1 to 1.15, it will be stable and as long as the maximum crest acceleration of the dam is less than 0.75 g, the dam will be sustainable under an earthquake of magnitude 8.5 and its deformations will be tolerably small. Paskalov [12,13] included pore water pressure in calculating the critical acceleration using the average pore pressure coefficient and applied the method to seismic analysis of the damages of Upper SanFernando dam by 1971 earthquake. It was concluded that the method predicts the permanent deformations successfully. Hynes-Griffin and Franklin [14] stated in a report prepared for a group of engineers that if a dam is designed for an acceleration equal to half the maximum acceleration at the dam base and has at least 1 m additional freeboard, it will remain stable if a safety factor of at least one is reached using undrained parameters. Finn et al. [15] developed the TARA-3 computer program and directly calculated permanent deformations. The program was capable of performing both dynamic and

static analysis using either effective or total stress conditions. Daghigh [16] conducted a numerical study on the dynamic behavior of earth dams under seismic loading, and the general differential equation of dynamic equilibrium was solved using three different methods: 1) modal method, 2) complex response method, and 3) implicit numerical integration method. Cai and Bathurst [17] reviewed two methods, including one which only uses the peak ground acceleration and velocity as the properties of input motion and the other method which uses the fundamental period of the acceleration and provides the probability of exceedance for the expected permanent displacement. They indicated that statistically, the second method provides more reliable results. Matsumoto [18] conducted shaking table experiments involving models with maximum accelerations up to 0.7g. These experiments showed that only shallow landslides without deep and distinct failure surfaces in the core occur. Therefore, it was concluded that the Newmark method may be somewhat unrealistic. Day [19] demonstrated theoretically that slopes made of dry granular soil can undergo settlements and lateral deformations under an earthquake with a peak ground acceleration less than the critical acceleration. Therefore, he concluded that in some cases the Newmark method may not be reliable. Swaisgood [20] investigated over 70 earthquake-induced failures. The results showed that the peak ground acceleration (PGA) and earthquake magnitude ( $M_w$ ) are the most important factors affecting the crest settlement of dams due to earthquakes. A graph was developed that briefly summarizes the relationship between the measured settlement and the maximum ground acceleration. A new empirical relationship was also presented. It was also found that the deformations of the dam were mainly settlement and lateral deformation, and no sliding along a distinct failure surface was observed. Based on the investigations, serious damages to the dam was only observed in cases where the PGA exceeded 0.2g, which was consistent with previous findings that a well-constructed dam can withstand moderate earthquakes with a maximum acceleration of up to 0.2 without damage. Wang et al. [21] incorporated a new nonlinear, effective-stress-based bounding surface hypo-plasticity model for sand instead of the frequently used the equivalent linear approach. They calculated permanent deformations and compared with the values estimated using other used models and measurements and concluded that the results showed the role of a suitable constitutive equation. Han and Hart [22] compared simple elastoplastic models with equivalent linear models and nonlinear numerical methods and concluded that simple elastoplastic models with small damping are accurate enough to determine the permanent settlements at the dam crest. Bray and Travasarou [23] utilized a nonlinear fully coupled stick-slip sliding block model to simulate the dynamic performance of an earth dam. The seismic displacement model which was developed capture the yield coefficient  $k_y$ , initial fundamental period  $T_s$ , and the ground motion's spectral acceleration at a degraded period equal to  $1.5T_s$ , and includes the simultaneous occurrence of the nonlinear dynamic response of the potential sliding mass and the effects of periodic sliding events. The proposed model provided estimates of seismic displacements that were generally consistent with documented cases of earth dams. Sica et al. [24] studied the seismic performance of a zoned earth dam using coupled analysis. It was revealed that previously experienced stress paths, such as strong motions, influence seismic performance by hardening of the soils. The hardening parameters could be obtained by back analysis of a seismic event. Rampello et al. [25] evaluated the response of a homogeneous earth dam under real and synthetic earthquake loadings assuming different depths of bedrock. They conducted decoupled approach of displacement-based analysis which is based on the assumption that the sliding block analysis can be decoupled from the ground response analysis of the earth structure. They concluded that permanent displacements are resulted from plastic strains that accumulate during the earthquake because of the progressive plastic loading which are influenced by the duration of the strong

motions. Also, the results showed that the horizontal and vertical displacements of the body were also less than the crest settlement due to the mobilization of shear resistance in the confined upper third of the dam. The results of the finite element analysis were also higher than those of the double integration method from the acceleration diagram. Jinto and Davidson [26] compared the existing methods for determining permanent earthquake-induced displacements. They also critically reviewed the pseudo-static method and showed that the effective stress dynamic analysis method is a perfect tool for assessing the impact of earthquakes on earth dams, particularly their permanent deformations. Jibson [27] compared different methods for calculating permanent displacements and concluded that the rigid block analysis method is more suitable for shallow landslides and stiff ground. In contrast the coupled sliding block method is more suitable for deep landslides and softer soils. Also, it was concluded that the sliding block method is suitable for cases where the soil fundamental periods are greater than 10% of the average earthquake periods. Hsieh and Lee [28] modified the relationship between critical acceleration, Arias earthquake intensity, and permanent displacements by considering various sites and adding a new term, proposing more accurate relationships for rock and soil sites. Davoodi et al. [29] investigated the effect of fundamental periods of dam on the crest settlement of the dams in near or far field earthquakes. They indicated that high dams have smaller settlement of the crest and more critical responses to near-field records and shorter dams have more critical responses to far-field records. Dong et al. [30] investigated an ultra-tall dam and found that the acceleration amplification in the upper part of the dam increases sharply and reaches a maximum at the crest, and horizontal and vertical displacements at the crest are the largest. Bandini et al. [31] proposed a more complete method that considers the changes in wedge geometry and shear resistance due to sliding. The predicted behavior matched the observed behavior, which indicates the need to consider changes in block geometry and shear resistance due to sliding in the calculations. Park and Kutter [32] studied the effects of soil sensitivity on slope failure mechanisms by performing some static and dynamic centrifuge experiments for different earthquake input motions and some Vane shear and uniaxial compression tests to obtain the strength and sensitivity of the materials. It found that in dynamic tests, in a deep failure, there exists a diffused plastic zone, while in a shallow failure distinct shear bands are formed. Bray et al. [33] proposed a new probabilistic method incorporating the uncertainty of input ground motion. This model considers the slope's strength, vibration characteristics, and earthquake intensity. Ghahraman-nejad and Kan [34], using various methods of analysis ranging from empirical to non-linear numerical, compared the deformations of several case studies and predicted the magnitude of the crest settlements and concluded that assuming a unique failure plane, as adopted by some of the simplified methods, may be necessarily misleading, as deformation would be more likely to be characterized by the deformation pattern predicted using a non-linear elastoplastic model and numerical modeling. Chen and Liu [35] used Choleski decomposition method to generate random field for spatial variability of porosity and quantified a relation between the compaction quality and porosity. Implementing the relation in stochastic finite element method, it was concluded that the spatial variation of the compaction quality will lead to significant risk of exceeding standard of the displacements and stresses. Rollo and Rampello [36] employed a probabilistic approach to analyze slope stability during earthquakes with the ability to incorporate the inherent variability. The analysis exploits a comprehensive database of ground motion measurements. Mazaheri et al. [37] presented an improved approach by employing both static and dynamic analyses and an elastoplastic model, and Rayleigh damping in Abaqus software and studied the Azadi dam. The results of the dynamic analysis showed a 37% increase in settlement compared to the quasi-static

analysis. Cho and Rathje [38] developed a generic predictive model for earthquake-induced slope displacements based on the results of many of nonlinear finite-element (FE) simulations. The model was the first that related the displacement with the ratio of the depth of the critical slip surface relative to the slope height. Hwang and Rathje [39] performed a numerical parametric analysis consisting several models with soil stiffness and strength parameters selected to isolate the impact of yield acceleration, depth of the sliding mass, natural period of the slope, and the slope angle on the deformation patterns. The results indicated that deeper sliding masses experience notable strain localization at the sliding mass depth, while shallow sliding masses experience more distributed straining throughout the entire soil mass. Also, larger displacements for the deep sliding masses relative to shallow sliding masses at small  $k_y$  are observed, whereas shallow sliding masses experience larger movements at large  $k_y$ . Zhang et al. [40] examined the combined effects of mainshocks and aftershocks on slope sliding using 273 ground motion records from actual seismic sequences. The calculation results were compared with the traditional Newmark method and a displacement predictive model based on the FEM was proposed. They concluded that the sliding displacements which are calculated based on considering the aftershock effect were more conservative compared to those that only considered the mainshock effect. Consequently, a combination of the optimal scalar parameter of the mainshock and an aftershock parameter is required to express the characteristics of the seismic sequence.

According to the literature review, the utmost important objective of the dynamic analyses performed is to examine the accuracy of past approximate methods and to compare them with the results of dynamic analysis based on the finite element method (FEM). Therefore, it is attempted to use the geometry and characteristics corresponding to those of the Ambraseys and Sarma [6] so that the results obtained under the same initial conditions can be compared. In this study, a finite element software was used to calculate the accelerations and an auxiliary software was developed to determine the average acceleration and displacement in any specific failure wedge based on the analysis results. As a case study, the procedure was performed on the Kheyraabad dam using its real geometry and geotechnical parameters.

## 2 Materials and methods

The results of three different classic methods of calculating permanent displacements of the dam were compared with the results of numerical methods. The classic methods include: Ambraseys-Sarm, Sarma, and Makdisi-Seed methods. These methods and their related factors are briefly reviewed here.

### 2.1 Ambraseys-Sarma method

In this method, a series of wedges are considered with different depths ranging from  $0.2h$  up to  $2h$  from the dam crest, where  $h$  stands for dam height. The considered wedges have a specific shape, which is defined by  $n$ , the ratio of wedge depth to dam height,  $\psi$ ,  $\theta$ , as shown Fig. 1. The ratio of maximum of average wedge acceleration to peak ground acceleration,  $\bar{k}_n$ , is maximized at a  $\theta$  about 50 when the wedge angle,  $\psi$ , is around 80 to 90. This increase in  $\bar{k}_n$  becomes less significant as the fundamental period of the dam increases.

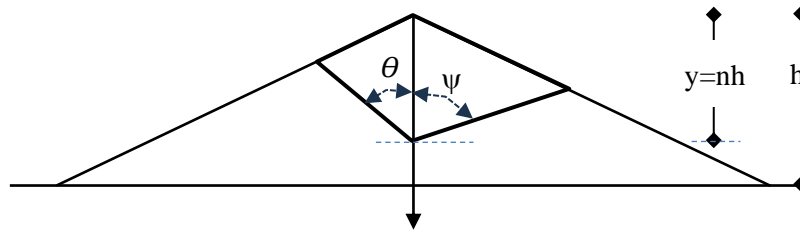


Figure 1. General Wedge geometry in Ambrasis & Sarma [6]

### 2.1.1 Natural Period of Vibrations of the Dam

In all of the methods of analysis, the natural frequency of the first mode of vibrations of the dam body should be determined, which can be calculated based on the Sarma method [41] as in equation 1:

$$T_0 = \frac{2\pi h}{S_1 a_1} \quad (1)$$

where  $h$  stands for the dam's height, and  $S_1$  is the shear wave velocity in the dam body. The coefficient  $a_1$  is obtained from Fig 2 based on the relative shear wave velocity in the foundation alluvium and the dam body parameters  $m$  and  $q$ , which are calculated using equations 2 and 3, presented in the following:

$$m = \frac{s_1 \rho_1}{s_2 \rho_2} \quad (2)$$

$$q = \frac{s_1 (H - h)}{s_2 h} \quad (3)$$

where  $H$  is the sum of the dam's height and the thickness of its alluvial foundation, and  $S_2$  is the shear wave velocity of the alluvial foundation of the dam. Also,  $r_1$  and  $r_2$  are densities of the dam body and its alluvial foundation, consequently.

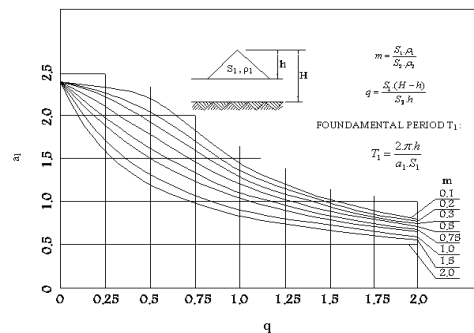


Figure 2. Fundamental period of the dam and foundation system [41].

As in the analyzed models the dams are assumed to be on seated on the bedrock, the value of  $q$  in Fig. 2 is zero and therefore, the value of  $a_1$  is 2.3. Based on the relation between elastic modulus and shear wave velocity, the relation between the natural frequency,  $T_0$ , and elastic modulus,  $E$ , can be written as in equ. 4:

$$T_0 = \frac{2\pi h}{S_1} \sqrt{\frac{2(1 + \mu)\rho}{E}} \quad (4)$$

where  $\rho$  is the density of the dam body materials. This shows that the natural period,  $T_0$ , is inversely proportional to the elastic modulus. Given the natural period of the dam body,  $T_0$ , the  $\bar{k}_n$  can be determined for any given wedge based on its  $n$ , which then can be multiplied by the peak ground acceleration to obtain the maximum simultaneous acceleration for the given wedge. Given  $\bar{k}_n$ , and the maximum ground acceleration,  $a_{\text{base,max}}$ , the maximum simultaneous earthquake force applied to the wedge,  $F_n$  can be obtained from equation 5:

$$F_n = M_n \cdot \bar{k}_n \cdot a_{\text{base,max}} \quad (5)$$

where  $M_n$  presents the mass of the wedge. In the next step, the critical acceleration,  $k_y$ , the acceleration at which the safety factor for a given wedge is equal to one, must be determined. The critical acceleration for any wedge is obtained from the equation 6:

$$k_y = tg(\varphi_{eq} - \alpha) \quad (6)$$

where  $\varphi_{eq}$  is the equivalent friction angle and  $\alpha$  is the slope of wedge. Using coefficient  $C$ , as calculated using equation 7:

$$C = \frac{\cos(\beta - \theta - \varphi')}{\cos \varphi'} \quad (7)$$

where,  $\beta$  indicates the average angle of the shear surface with the horizon,  $\theta$  is the angle of earthquake force with the horizon, and  $\varphi'$  is the effective friction angle of the material along the shear surface. Using  $k_n$  and the value of the coefficient  $C$ , the amount of horizontal displacement  $X_m$  can be calculated using the relevant graphs.

## 2.2 Sarma Method

The method of Sarma is mainly similar to the method of Ambraseys-Sarma, but in this method the charts modified by Sarma [7] are used. In this case, the maximum acceleration applied to the wedge can be calculated.

## 2.3 Makdisi-Seed Method

In this method, the first step is determining the maximum acceleration applied to the dam crest,  $\dot{U}_{\text{max}}$ . Determining the  $\dot{U}_{\text{max}}$  is difficult as it is very fluctuating. This is the weak point of the method. However, it can be determined using a finite element dynamic analysis. Next, the ratio of the maximum simultaneous acceleration applied to the intended wedge ( $K_{\text{max}}$ ) to the maximum acceleration of the dam crest can be estimated from the relevant charts based on the ratio of the wedge depth to the dam height. Then, the critical acceleration,  $k_y$ , the acceleration at which the safety factor of the wedge becomes equal to one, is calculated using pseudo-static analysis (SLOPE/W) or equation (6). Finally, the displacement induced in the intended wedge is determined using earthquake magnitude and the natural period of the dam body. [10]

## 2.4 Finite Element Method

In this study, the finite element method along with the nonlinear material behavior models were used for the dynamic analysis of the dam body. To perform the dynamic finite element analysis in the QUAKE/W software, first a preliminary static analysis must be performed to determine the initial stresses [42]. In this case, the required parameters are the elastic modulus, Poisson's ratio, shear modulus, and specific gravity of the materials. After the static analysis, the obtained stresses are used as input data for the dynamic analysis. In the stage of dynamic analysis, after introducing the initial static model as input, the functions of the variations of shear modulus and damping ratio, obtained from cyclic tests or existing charts, are entered. In this analysis, if a linear elastic model is used, the constant damping and shear modulus are used. Nevertheless, if an equivalent linear model is used for the material behavior, the damping ratio and shear modulus functions must be used [19]. Then, the results of the dynamic analysis of the models are used as input data in SLOPE/W. In this case, the calculated values of stress and strain in the dynamic analysis at each Gaussian point are used by the SLOPE/W calculations to estimate the failure wedge, average acceleration and displacement of the wedge, safety factor, critical acceleration of the wedge, etc.

### 2.4.1 Computational time step

The results of dynamic analysis calculations are sensitive to the choice of appropriate time step. The smaller the time step, the higher the accuracy of the results [42]. However, this needs much more time and computational cost. Therefore, to determine the appropriate time step, first the most significant frequency of loading or required response must be determined. If this value is denoted by  $\omega_n$ , based on equation (8), 5% of the corresponding period is considered as the time step, unless a smaller value for  $\Delta t$  is required due to convergence problems in the nonlinear analysis [42]:

$$\Delta t = \frac{1}{20} \frac{2\pi}{\omega_n} \approx \frac{0.3}{\omega_n} \quad (8)$$

## 2.5 Material properties and geometry of the dam in validation calculations

As the Sarma and Ambraseys (1967) models assume the dam's sections to be triangular and homogeneous, a homogeneous dam with a height of 50 meters and a side slope of 2.5H:1V is considered for validation calculations [6]. The characteristics of the model and the material properties used in validation calculations are presented in Table (1).

**Table 1. Material properties and geometrical parameters used in validation example**

Elastic Modulus (kPa)	105	Poisson Ratio	0.4
Natural Period (sec.)	1	Cohesion (kPa)	11
Damping (%)	20	$\theta$ of wedge(deg.)	50
Friction Angle (deg.)	38	$\psi$ of wedge(deg.)	90

Soil stiffness is generally a function of the stress state, and the soil stiffness increases with increasing confining or overburden stress. It is particularly true for non-plastic granular soils. QUAKE/W uses Equation (9) to implement this effect:

$$G = K_G \cdot (\sigma_m')^n \quad (9)$$



where,  $K_G$  and  $n$  are experimental constant coefficients and  $\sigma'_m$  is the average of the effective principal stresses. If the value of  $n$  is set equal to zero,  $G$  becomes a constant value, and if it is equal to one, then  $G$  increases linearly with depth. The value of the dynamic shear modulus,  $G$ , for the shell and core of the dam (granular and cohesive media) is obtained from equations 10 and 11 as follows:

$$G = 32700 \frac{(2.97 - e)^2}{4e} \sqrt{\sigma'_m} \quad (\text{used for dam core}) \quad (10)$$

$$G = 2210 K_2 \sqrt{\sigma'_m} \quad (\text{used for dam shell}) \quad (11)$$

Here, the shear modulus value,  $G$ , is obtained in kPa. The void ratio,  $e$ , based on the consolidation tests on samples prepared according to construction specification, is equal to 0.56 for core materials. The value of the coefficient  $K_2$  is a function of the induced shear strain on the soil, the relative density of the material, and the gradation of the granular material. It is presented by experimental curves, covering the design purposes and conditions where the loading duration is less than 4 to 10 seconds. It is assumed to be between 120 and 170, with an average of 150.

## 2.6 Details of the developed code

Performing dynamic analysis by QUAKE/W can yield the values of acceleration, displacement, etc. at each node [42]. However, to determine the sliding wedge, the dynamic model must be linked to SLOPE/W. Also, the average acceleration, critical acceleration, safety factor, and displacement of the critical wedge must be calculated using the Newmark method throughout the earthquake duration. To compare the classic pseudo-static and the finite element method, a program was written to calculate the items mentioned above for any specific wedge at each time step, based on the results of the finite element analysis [43]. This rectifies the weakness of continuum mechanics-based models in determining plastic deformations. In this program, first, the coordinates of the nodes of the generated mesh in the model are read from the QUAKE/W program. Then the components of displacement, velocity, and acceleration at each node in both  $x$  and  $y$  directions are read from the output of the dynamic analysis [44]. Next, the configuration of the dam, including the upstream and downstream slopes, height and width of the berm (if any), and the configurations of the intended wedge, including the slopes of the two broken lines, are entered. The program starts by identifying all points located in the intended wedge, and stores their information. Then, the wedge area is divided into horizontal strips, the number of which is specified by the user, and the nodes located in each strip are identified, and their average displacement and acceleration are calculated and stored as the average displacement and acceleration of the strip. Finally, the average acceleration of the wedge is obtained using equation (12):

$$\ddot{U}_{ave} = \frac{1}{A} \sum a_i \ddot{U}_i \quad (12)$$

where  $a_i$  is the cross-sectional area of the  $i^{\text{th}}$  horizontal strip,  $\ddot{U}_i$  is the average acceleration of the  $i^{\text{th}}$  horizontal strip calculated by the code, and  $A$  is the total cross-sectional area of the wedge. These steps are repeated for each time step. After each step, the final result is saved. Finally, the variations of maximum acceleration of the intended wedge are plotted as a function of time. In the next step, the developed code calculates the maximum displacement of the intended wedge at each time step by two different methods. In the first method, the same steps which were used to

calculate the maximum average acceleration are followed. In this method, equation (13) is used to calculate the maximum displacement of the wedge:

$$U_{ave} = \frac{1}{A} \sum a_i U_i \quad (13)$$

where the  $U_i$  is the average displacement of the  $i^{\text{th}}$  horizontal strip. This method is used when the wedge behaves elastically, and has not yet entered the plastic state. To determine the behavior of the wedge, the shear stresses in the dam body are determined after completing the dynamic analysis. Also, the shear resistance at the bottom of the wedge is calculated using the Mohr-Coulomb shear strength model as in equation 14:

$$\tau_{max} = c' + \sigma'_n \tan(\phi') \quad (14)$$

where  $c'$  is the effective cohesion,  $\sigma'$  is effective vertical stress, and  $\phi'$  is the effective friction angle. If  $\tau_{max}$  is less than the working shear stress, the permanent deformations in the wedge have occurred, otherwise, the deformation of the wedge is considered elastic. In the second method, after calculating the average maximum acceleration applied to the wedge and plotting it as a function of time by double integration of the part of the acceleration-time curve in terms of time which is higher than the critical acceleration, the average maximum displacement of the wedge is obtained, which is the permanent displacement of the wedge.

### 3. Results and discussion

#### 3.1 Validation Calculations

As mentioned in the previous section, a practical example was used in order to ensure the accuracy of the results of the model. The El Centro earthquake accelerogram was selected as the input earthquake to the model, and the boundary conditions were also defined. It was assumed that the dam is seated directly on the bedrock, which means that the entire bottom boundary of the model was assumed to be fixed in both x and y directions. Figure (3) shows some of the wedges used in the validation stage. Also, a summary of the results obtained from the methods mentioned above, is presented in Table 2.

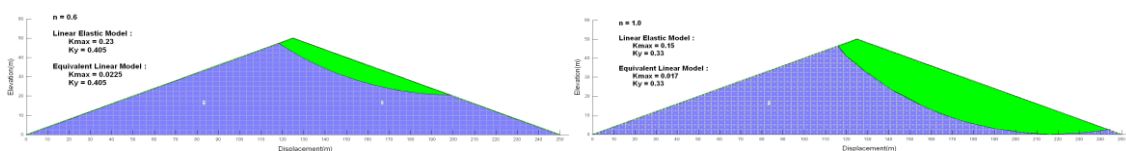


Figure 3. Maximum acceleration and critical acceleration in wedges used in validation stage.

As can be seen in Fig. (3), the shape of the wedges formed in the dam's body was entirely different from what Ambraseys and Sarma [6] had considered as the critical wedge. Therefore, the average critical acceleration of the wedges did not follow the graphs presented by Ambraseys and Sarma [6]. In order to reduce the number of variables and simplify the calculations, the shape of the critical wedge was adopted based on the graph prepared by Ambraseys and Sarma [6], which is inherently unable to yield accurately the acceleration induced in trial wedges with arbitrary shape. As can be seen in Table 2, among the classic methods, the Ambraseys-Sarma method [6] has resulted in the highest maximum horizontal accelerations and the lowest

maximum displacements, and it differed significantly from the other two methods. However, the results of the Sarma and Seed-Makdisi methods, which show lower maximum accelerations and larger maximum displacements, are closer to each other. However, the difference between these two methods is significant for shallow wedges, while for the case of wedge depth equal to dam height, they are very close. The main reason of the difference in the results of the Ambraseys-Sarma method with other two methods, is the method of determining the critical acceleration. This result indicates the importance of choosing the strength parameters, especially for the shell zone, as it controls the critical acceleration. Also, according to Tab.3, the calculated displacements from the classic methods and the numerical dynamic analysis performed with the linear elastic model using SLOPE/W are much greater than the other methods.

**Table 2. Summary of dynamic analysis results of classic methods for validation example**

Wedge Depth	Maximum Displacement (m)			Critical Acceleration (g)			Maximum Acceleration (g)		
	1	2	3	1	2	3	1	2	3
0.2h	0.97	0.480	0.63	0.014	0.240	0.014	0.418	0.530	0.460
0.4h	0.78	0.140	0.59	0.011	0.240	0.011	0.300	0.456	0.357
0.6h	0.52	0.040	0.42	0.012	0.240	0.012	0.209	0.342	0.272
0.8h	0.27	0.008	0.25	0.020	0.240	0.020	0.165	0.275	0.0204
1.0h	0.14	0.000	0.15	0.025	0.240	0.025	0.119	0.216	0.150

1=Sarma, 2=Ambraseys-Sarma, 3=Seed-Makdisi

One of the reasons for this is the use of a linear constitutive model for the soil. The energy dissipation in plastic deformations is not considered in this model. Unfortunately, most classic methods are based on a linear elastic model for soil materials. Linear numerical dynamic analysis is only suitable for relatively rigid structures subjected to low vibrations. In soil structures where the elastic zone of materials is very limited, usually nonlinear analysis is necessary.

**Table 3. Summary of dynamic analysis results of numerical methods for validation example**

Wedge Depth	Maximum Displacement (m)				Critical Acceleration (g)				Maximum Acceleration (g)			
	SlopeW		Code		SlopeW		Code		SlopeW		Code	
	1	2	1	2	1	2	1	2	1	2	1	2
0.2h	0.845	0.149	0.124	0.0640	0.014	0.014	0.014	0.014	0.420	0.034	0.684	0.294
0.4h	0.784	0.129	0.110	0.0636	0.011	0.011	0.011	0.011	0.295	0.028	0.512	0.290
0.6h	0.707	0.089	0.095	0.0630	0.012	0.012	0.012	0.012	0.230	0.023	0.447	0.292
0.8h	0.504	0.000	0.079	0.0615	0.020	0.020	0.020	0.020	0.180	0.020	0.429	0.297
1.0h	0.365	0.000	0.063	0.0544	0.025	0.025	0.025	0.025	0.150	0.017	0.376	0.289

1= Linear model, 2=Equivalent Linear model

Another notable point is that the written code, which uses the results of the QUAKE/W program at each time step, gives more realistic figures. Table 4 presents relatively similar measured values. All of these figures indicated the validity of the calculations of the written code. This shows that classic and numerical methods based on elastic behavior are very conservative and lead to extra volume of construction operations, materials consumption, and construction costs. Therefore, numerical methods and more accurate constitutive models must be used.

### 3.2 Kheyrahad Dam Calculations

In this research, the Kheyrahad dam was used as a case study. The dam site is located 33 km south of Behbahan city, near the Behbahan-Bandar e Deylam asphalt road, on the Kheyrahad Table 4. A history of some of the permanent displacement incidents occurred in a number of dams in different countries

No. Dam properties			Earthquake Properties						Damage			
Name	Country	Type	H (m)	CL (m)	FT (m)	date	M	FD (km)	PGA (g)	S. (m)	Damage	
1	Vermilion	California	E	50	1290	50	80.05.27	6.3	22	0.24	0.05	Negligible
2	Namioka	Japan	ECRD	52	265	0	83.05.26	7.7	145	0.08	0.06	Negligible
3	La Villita	Mexico	ECRD	60	427	75	85.09.21	7.5	61	0.04	0.12	Negligible
4	Nagara	Japan	ECRD	52	-	?	87.12.17	6.9	29	0.27	0.02	-
5	Austrian	California	E	56	213	0	89.10.17	7.1	2	0.57	0.85	Sever
6	Lexington	California	E	63	253	0	89.10.17	7.1	3	0.45	0.26	Minor
7	Diayo	Philippines	ECRD	60	201	0	90.07.16	7.7	18	0.38	0.07	Minor
8	R. Matthews	California	E	46	192	0	92.04.25	6.9	64	0.07	0	Negligible
9	Los Angeles	California	E	47	671	0	94.01.17	6.7	10	0.43	0.09	Medium

**E: Earthfill dam, ECRD: Earth Core Rockfill Dam, H: Height, CL: Crest Length, FT: Foundation Thickness, M: Magnitude, FD: Focal Depth, PGA: Peak Ground Acceleration, S: Crest Settlement river.**

This river is a tributary of Zohreh river. The dam is an earthfill-rockfill dam with a vertical clay core, a height of 60 meters from the foundation, a crest length of 720 meters, and a body volume of 4.5 MCM. The reservoir volume equals 179 MCM, the normal reservoir level is 259.6 meters above sea level, and a maximum flood level of 269.5 meters above sea level.

#### 3.2.1 Design Earthquakes

Since the graphs provided in currently available methods are based on the El Centro earthquake accelerogram, this earthquake was used in numerical analysis of this research, in order to obtain comparable results. However, for dynamic modeling of the dam, the seismological characteristics of the construction site should be used. By combining the seismologic and geological studies of the site, the acceleration with a specified occurrence probability over the structure's life is calculated based on statistical methods. The horizontal component of acceleration of the design base level (DBL) earthquake is 0.295 g, and the vertical component is 0.18 g. The horizontal component of accelerations of the maximum design level (MDL) earthquake is 0.406 g, and the vertical component is 0.253 g.

#### 3.3.2 Dynamic analysis of Kheyrahad dam using classical methods

In this stage, the stability of the Kheyrahad dam (Fig. 4) under earthquake conditions is investigated using the pseudo-static method. In this context, slope stability analysis is performed using the limit equilibrium method, and the effect of the earthquake is implemented by horizontal or vertical forces, or both applied to the center of gravity of each slice. The magnitude of these forces were calculated by multiplying the seismic coefficients to the weight of each slice. In other words, in this analysis, a fraction of the acceleration of gravity is considered as the equivalent seismic inertia [45].

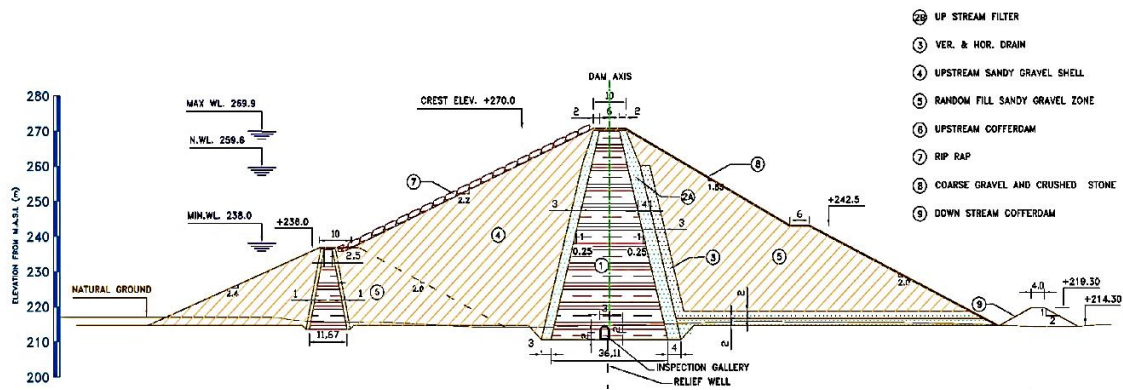


Figure 4: Geometry of highest cross-section of Kheyrahad dam

As during an earthquake, the displacement of the slopes of an earth dam is within an acceptable range, applying seismic coefficients corresponding to the probable earthquake at the site will result in the design of a slope that will not move or deform during the earthquake, which is unnecessary and very conservative [46]. On the other hand, the maximum acceleration of the probable earthquake is applied to the dam only for a fraction of a second, and then it will reduce or even change direction. Therefore, in practice, it is feasible to reduce the design seismic coefficient and accept some level of movement of the slope and its consequent deformation of the dam's body. The effective seismic coefficient is selected based on the magnitude and peak ground acceleration of the expected earthquake at the dam site. Usually, mandatory codes of practice require selection of some recommended seismic coefficients for dam design. Due to the lack of such criteria in the current dam design standards in Iran, the seismic coefficient in slope stability calculations is generally selected based on engineering judgment and with reference to technical manuals and codes of practice of other countries. For example, the Japanese standard recommends a minimum seismic coefficient of 0.18g at the foundation of dams in high-risk areas, which increases linearly to 0.45g at the dam crest. The US Army Corps of Engineers recommends a seismic coefficient 0.15 for high-risk zones in zoning maps.

Based on the above, and the results of seismologic studies of the Kheyrahad dam site, a horizontal seismic coefficient of 0.15 was used for the end-of-construction loading case and 0.15 and 0.20 for the remaining loading cases in the pseudo-static analyses. Due to the low and also unknown effect of the vertical component of earthquake, it was not applied. According to the results of the stability control analyses, in which accelerations of 0.15g and 0.2g were used as the PGA of the design base earthquake (DBE) and maximum credible earthquake (MCE), the studied storage dams will not have large and destructive deformations during an earthquake. During the occurrence of the maximum probable earthquake and the design base earthquake in short periods, the sliding masses will have an acceleration higher than the critical acceleration of the intended wedge. This acceleration, due to the reciprocating nature of the earthquake, changes direction immediately. However, a permanent displacement of the slopes of the dam occurs. These displacements must not compromise the overall stability of the dam. It means the deformations must be small, and give enough opportunity for the remediation process. The Newmark method, which calculates the permanent displacement of a specified wedge by double integration of the average acceleration of the sliding wedge in excess of the critical acceleration, has been used here. The methods proposed by Sarma, Ambraseys-Sarma, and Seed-Makdisi are used in this regard. According to seismological studies, the horizontal and vertical peak ground accelerations of the maximum credible earthquake at the Kheyrahad dam site were proposed to

be 0.532 g and 0.331, respectively. Assuming that the upstream shell is submerged, the downstream shell unsaturated, and the dam core is saturated, the average effective stresses in these zones are calculated using weighted averaging along the vertical slices, which were equal to 320, 400, and 664 kPa, respectively. As a result, the corresponding shear modulus values were calculated to be 589, 663, and 218.5 MPa, respectively. To calculate the average shear wave velocity in the dam body, weighted averaging of the shear modulus,  $G$ , and density,  $\rho$  were performed over the areas of each zone. Considering that the shear wave velocity for the upstream shell, downstream shell, and core were calculated to be 164, 183, and 102 m/s, respectively, the average shear wave velocity in the body is calculated to be 164 m/s. Therefore, considering that in this stage, the dam is assumed to be located on the bedrock, the value of  $q$  in the relevant charts will be zero, and as a result, the value of  $a_1$  is equal to 2.3. Using the values of  $h$ ,  $S_1$ , and  $a_1$  the natural period of the first mode of vibration of the dam body was estimated to be 1.0 second. Using the Ambraseys-Sarma chart, the natural period of the dam body, and the maximum bedrock earthquake acceleration, the maximum acceleration induced at the dam crest is calculated to be 0.66g. The results of dynamic calculations show that despite the material damping, due to the bottom-up propagation of transverse earthquake waves, the wave vibrations are amplified along the dam's height dam.

To calculate the earthquake permanent displacements, initially, the critical seismic coefficient must be determined. For this purpose, sliding surfaces for different depths have been analyzed using the SLOPE/W software. As mentioned in earlier, various methods has been used for this purpose, including the Ambraseys-Sarma, the Sarma, and the Seed-Makdisi methods. The results of these methods are presented in Tab. 5:

**Table 5. The calculated permanent displacements of Kheyrabad dams using 1) Sarma, 2) Seed-Makdisi, 3) Ambraseys-Sarma methods**

Wedge Depth (y/h)	Kc			Km			Kc/Km			$\frac{4X_m}{C \cdot K_m \cdot g \cdot T^2}$			Xm (cm)		
	1	2	3	1	2	3	1	2	3	1	2	3	1	2	3
0.2	0.46	0.46	0.48	0.64	0.71	0.81	0.72	0.65	0.59	0.040	0.010	0.08	7.2	6.9	18.0
0.4	0.30	0.30	0.43	0.45	0.50	0.70	0.67	0.60	0.62	0.053	0.011	0.07	6.8	5.2	13.8
0.6	0.29	0.29	0.41	0.32	0.42	0.52	0.91	0.69	0.79	0.001	0.006	0.02	0.1	2.6	2.9
0.8	0.29	0.29	0.4	0.25	0.31	0.42	1.16	0.93	0.95	-	0.0002	0.001	0.0	0.0	0.1
1.0	0.24	0.24	0.38	0.18	0.23	0.33	1.33	1.04	1.15	-	-	-	0.0	0.0	0.0

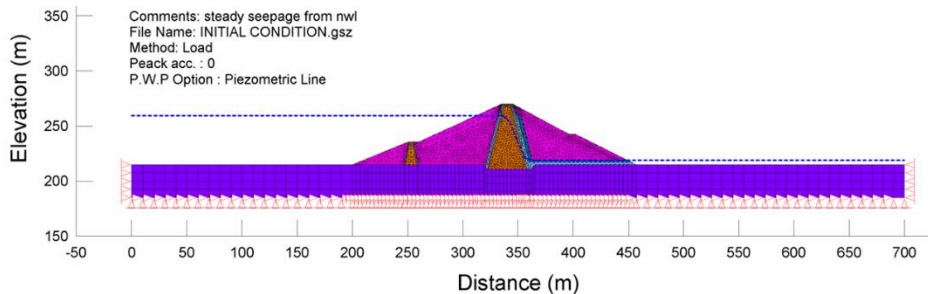
### 3.3.3 Dynamic analysis of Kheyrabad dam using numerical methods

For the dynamic analysis of the Kheyrabad earth dam, first, the static stresses were determined using appropriate linear elastic geotechnical properties of the materials, as presented in Table 6, which were introduced to the QUAKE/W sub-module of Geo-Studio finite element software. The discretization of the dam is presented in Fig. 5, and contour lines of calculated initial static stresses is presented in Figs. 6, which proves the validity of the numerical calculations. Next, the Naghan earthquake accelerogram, scaled to the design maximum probable earthquake (MDL) acceleration, presented in Fig. 7, was used, and the dynamic calculations were performed.

**Table 6: The geotechnical material properties used in initial static analysis**

Material	Saturated density	Wet density	Elastic Modulus	Poisson ratio	Shear Modulus	Damping ratio
	$\gamma_{sat}$ Ton/m <sup>3</sup>	$\gamma_{wet}$ Ton/m <sup>3</sup>	E MPa	$\nu$	G MPa	$\xi$ (%)
Shell	2.19	1.98	58	0.32	22	0.10
Filter	2.16	2.00	40	0.34	14.9	0.15
Core	2.10	2.02	20	0.36	7.35	0.20
Foundation	2.20	2.20	2000	0.30	76.9	0.02

Nevertheless, for the equivalent linear model, instead of the constant values provided in table 5, the damping ratio and shear modulus were selected based on shear strain and according to the functions shown in Figure 8. The time step in calculations was chosen iteratively. The peak horizontal accelerations of Kheyribad Dam under the El Centro earthquake scaled to a maximum acceleration of  $g$  0.41 were calculated for time steps of 0.01, 0.02, 0.05, and 0.08 sec. The results were significantly different when 0.08 sec was used for the time step, but the same results were obtained when 0.01 and 0.02 sec were used as time steps. Considering saving in time and cost, and ensuring the accuracy of the solution, the time step of 0.02 sec was used in all analyses.

**Figure 5: The discretization and boundary conditions of Kheyribad dam**

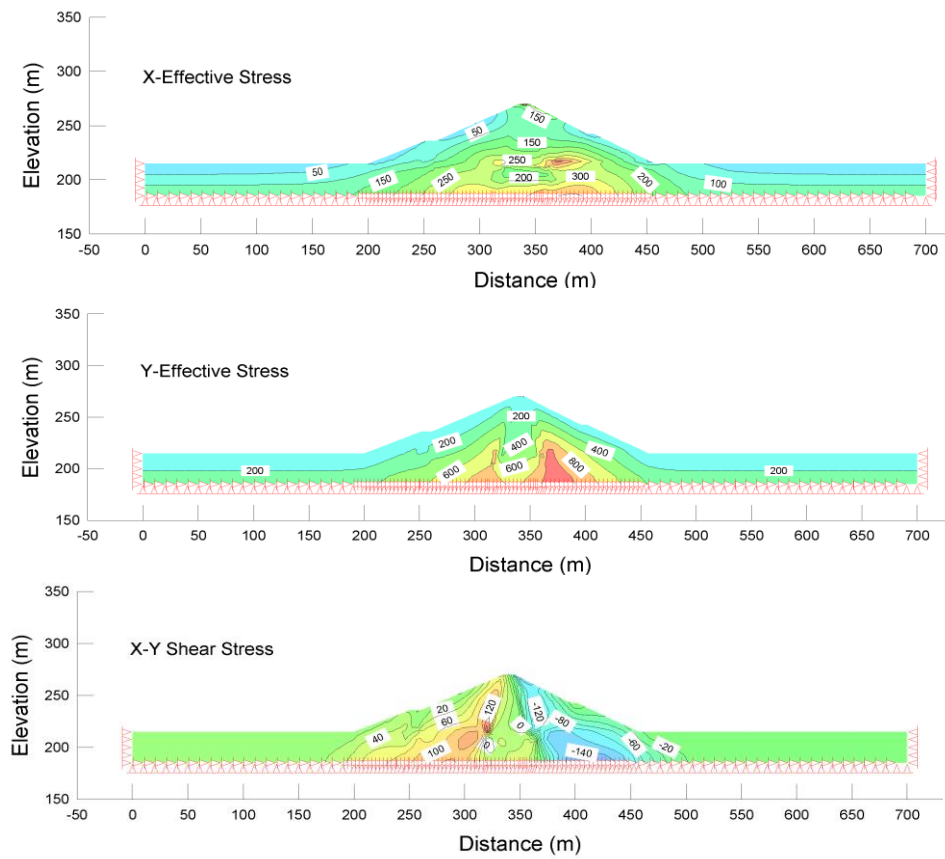


**Figure 6: Isometric contour lines of the initial static stresses of Kheyrabad Dam**

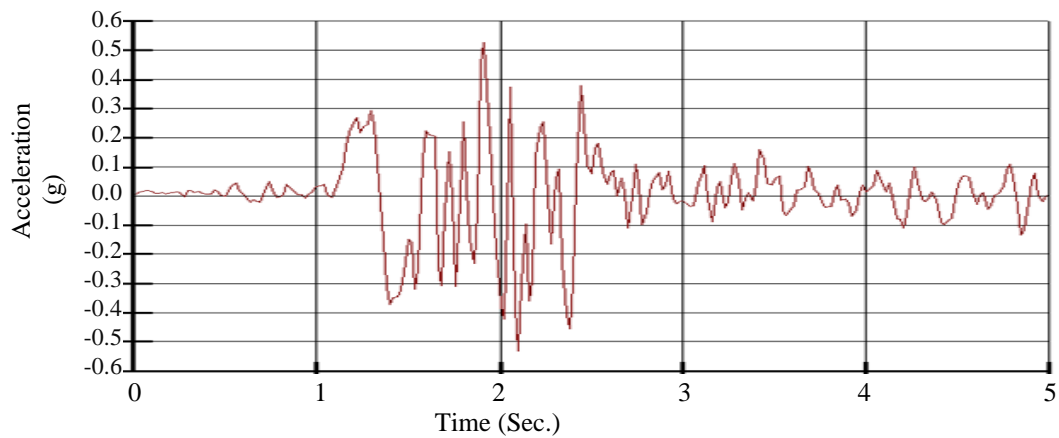


**Figure 7: Naghan earthquake record scaled to MDL earthquake of Kheyrabad dam**



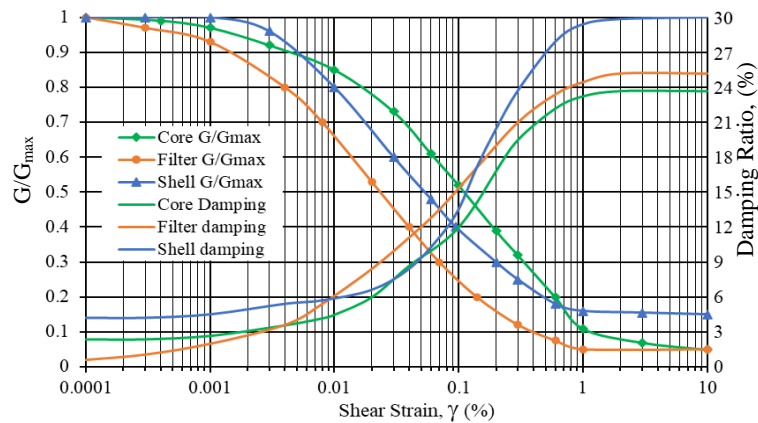


**Figure 8: Shear modulus and damping ratio functions for dynamic analysis**

The results of the dynamic analysis were used to determine the average acceleration and displacement induced in any intended wedge. The stresses, accelerations, and displacements calculated by the dynamic analysis were imported to the SLOPE/W software. It calculates the average acceleration and displacement for the intended wedges using the Newmark method. The final results of the dynamic analysis for wedges with different depths are summarized in Table 7, which presents the results of the dynamic analysis for both linear elastic and equivalent linear models.

It is observed that although the maximum acceleration at the dam crest was higher in the linear elastic model than in equivalent linear model, the maximum displacement obtained in this model was less. This was attributed to the decrease in the shear modulus ratio with increasing shear strain. Also, due to the increase in the damping ratio due to the increasing shear strain in the equivalent linear model, the dam crest accelerations were less than the elastic linear case model.

### 3.3.4 Dynamic analysis of Kheyraabad dam using numerical methods and the developed code

As the Newmark method is also a classic method, an effort was made to develop a program which could calculate the accelerations and displacements of wedges based on the results of the finite element method dynamic analysis.

**Table 7. Summary of the results of the dynamic stability analysis of Kheyraabad Dam performed with SLOPE/W**

Type of analysis	Wedge depth/dam height	0.2	0.4	0.6	0.8	1.0
Linear Elastic	Critical acceleration (g)	0.46	0.30	0.31	0.29	0.24
	Maximum acceleration(g)	0.24	0.23	0.21	0.19	0.17
	Displacement (m)	0.000	0.000	0.000	0.000	0.000
	Factor of Safety	1.55	1.35	1.20	1.19	1.15
Equivalent Linear	Critical acceleration, ky	0.38	0.25	0.29	0.23	0.18
	Maximum acceleration, kmax	0.069	0.062	0.050	0.044	0.040
	Displacement (m)	0.000	0.000	0.000	0.000	0.000
	Factor of safety	2.12	1.61	1.58	1.56	1.50



A summary of the results obtained by this code using both linear elastic and equivalent linear models is presented in Table 8. Also, a summary of the results of all methods including results earlier presented in tables 5, 7 and 8, is now presented in Table 9 for comparison. Figure 9 shows the variations of the permanent deformations calculated by the developed code for a wedge of 1.0h depth for both linear elastic and equivalent linear elastic models.

**Table 8. Summary of the results using the developed code for Kheyabad dam**

Type of analysis	Wedge depth/dam height	0.2	0.4	0.6	0.8	1.0
Linear Elastic	Critical acceleration (g)	0.46	0.30	0.31	0.29	0.24
	Maximum acceleration(g)	0.449	0.441	0.447	0.532	0.450
	Displacement (m)	0.000	0.028	0.021	0.024	0.036
Equivalent Linear	Critical acceleration, ky	0.38	0.25	0.29	0.23	0.18
	Maximum acceleration, kmax	0.559	0.557	0.541	0.528	0.555
	Displacement (m)	0.018	0.040	0.034	0.038	0.041

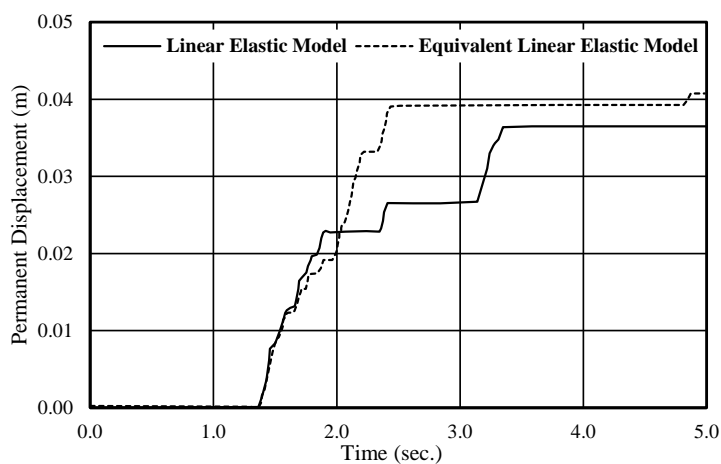


**Figure 9. Permanent displacements of a wedge of 1.0h height of Kheyabad dam under Naghan scaled earthquake**

**Table 9. Comparison of calculated acceleration and displacement in Kheyrabad Dam using different methods**

Analysis Method	Wedge Depth	Maximum Acceleration (g)	Critical Acceleration (g)	Maximum Displacement (cm)	Analysis Method	Maximum Acceleration (g)	Critical Acceleration (g)	Maximum Displacement (cm)
Sarima	0.2h	0.64	0.46	7.2	quake/w Linear Elastic Model	0.24	0.46	0.0
	0.4h	0.45	0.30	6.8		0.23	0.30	0.0
	0.6h	0.32	0.29	0.10		0.21	0.31	0.0
	0.8h	0.25	0.29	0.0		0.19	0.29	0.0
	1.0h	0.18	0.24	0.0		0.17	0.24	0.0
Ambraseys – Sarima	0.2h	0.81	0.48	18.0	Linear elastic and developed code	0.449	0.46	0.0
	0.4h	0.70	0.43	13.8		0.441	0.30	2.8
	0.6h	0.52	0.41	2.9		0.447	0.31	2.1
	0.8h	0.42	0.40	0.1		0.532	0.29	2.4
	1.0h	0.33	0.38	0.0		0.450	0.24	3.6
Seed- Makdisi	0.2h	0.71	0.46	6.9	Equivalent Linear and developed code	0.559	0.38	1.8
	0.4h	0.50	0.30	5.2		0.557	0.25	4.0
	0.6h	0.42	0.29	2.6		0.541	0.29	3.4
	0.8h	0.31	0.29	0.0		0.528	0.23	3.8
	1.0 h	0.23	0.24	0.0		0.555	0.18	4.1

As it can be seen in table 7, the results of the calculations using the developed code are significantly different from the results of classic methods and are lower than them. Also, the results of the equivalent linear model are more accurate and closer to the measurements. Fig. 8 shows that till the 1.9 sec time (between 1.7 and 2.1 sec), the permanent displacements in the equivalent linear model is close but less than the results of linear elastic model. However, after that, the results of permanent displacements of the equivalent linear model increases and becomes higher than the results of the linear elastic model. The developed code was used for calculations in both cases. This was due to the fact that the levels of strains induced in the dam body grew in the time range of zero to about 1.9 seconds were very low. On the other hand, according to the fig. 7, the shear modulus functions of the dam body materials start dropping after a specific strain, and the shear modulus decreases rapidly afterwards. Also, the strains in the intended wedge of the dam body, at about 1.9 seconds, correspond to the strains at which the shear modulus curve drops rapidly. It worths to note that the reason for the variability of the time of start of this changes between 1.7 and 2.1 seconds for different intended wedges is the changes in percentage of different materials constituting the wedges. A high ratio of the shallow wedges bodies consists of the core materials, but this ratio decreases gradually as the depth of the wedges increases and the percentage of the shell materials increases. Therefore, in shallow wedges, as the shear modulus of core materials starts reducing at higher strains compared to shell material, the time the equivalent linear permanent displacement exceeds the elastic linear permanent displacement is longer, 2.1 sec. However, in deep wedges, where the wedge body material is consists of the shell material, this time is reduced to 1.7 seconds.

Another point obtained from the tables is that the amount of displacement in the different classic and numerical methods differs. The calculated displacements in the models are all within the range of low displacements, but what is important is to note that when displacement occurs in a wedge, the safety factor of that wedge will be less than one. At same time, the safety factor obtained in numerical methods is very high and sometimes more than two.

On the other hand, based on the results obtained, it was found that despite the higher maximum acceleration applied to the dam crest in the linear elastic model, the crest displacement in this model is less than the equivalent linear model. The reason for this observation is the decrease of the shear modulus ratio and increase in damping ratio versus increasing shear strain.

In the linear elastic model, the damping ratio and shear modulus are constant. However, in the equivalent linear model, the damping ratio increases with strain, as a result of which, the accelerations of the dam crest decrease, on the other hand, the ratio of shear modulus decreases with strain, which increases the displacement of the dam crest in this model as compared to the linear elastic model. In the equivalent linear model, the displacement of the dam crest increases initially but subsequently decreases. This is attributed to using the damping function in the equivalent linear model instead of a constant damping. The results showed that the shape of the wedges formed in the dam body is entirely different from what Ambraseys and Sarma [6] proposed as the critical wedges. Therefore, the average critical acceleration of the wedges will not be consistent with the results of this method either. It may be worth mentioning that Ambraseys and Sarma [6] proposed this shape of the critical wedge in order to reduce the number of the variables, and to simplify the calculations. The results of the Sarma, Seed-Makdisi, Newmark (SLOPE/W), and finite element methods are presented separately in Table 9. It was observed that the displacements obtained from the classic methods, and the elastic linear model in the dynamic analysis performed using SLOPE/W, are very high. One of the reasons for this is the use of a linear elastic model for the soil. Majority of the classic methods are based on assuming a linear elastic model for soil materials. While the linear dynamic analysis is suitable only for structures consisted of stiff materials and subjected to low vibrations amplitudes. The domain of elastic behaviour of soil material is very limited, and nonlinear analysis is necessary. This finding is in agreement with the findings of some previous studies such as [47], [48] and [49]. Another considerable point in Table 9 is the significant difference between the results of the equivalent linear model in the SLOPE/W analysis and the analyses performed using the developed code. The classic methods widely used so far have been very conservative, leading to an increase in the time and costs of construction work. This highlights the need to use numerical methods and more accurate constitutive models.

#### 4. Conclusions

In the linear elastic model, the displacements increase with the increase in natural period and decrease in the material stiffness. Nevertheless, in the equivalent linear model, the displacements depend on the shear modulus and damping ratio which depend on strain level. As the equivalent linear model represents the behavior of soil materials more realistically, it is crucial to determine the strain-dependent shear modulus and damping ratio functions.

In homogeneous dams, the average of accelerations calculated by all different methods is higher for more shallow wedges and decreases with increasing the wedge depth. However, for non-homogeneous dams which include core, shell, and filter zones, the average acceleration of the wedge depends on the wedge location and the materials it passes through due to the different damping ratios of these materials.

The results of classic methods are often overestimated, leading to significant increase in the project construction time and cost.

The results proved that the Ambraseys-Sarma method yields very unrealistic estimates of the maximum acceleration applied to a wedge of a given depth. In Ambraseys-Sarma method it is assumed that the wedges pass through the center of the dam and consequently through the core, while analyses show that most of the wedges pass through the downstream shell, posing less threat to dam integrity. This is particularly important in dynamic analysis. The calculated permanent displacements of the Kheyrabad Dam under the design base earthquake for wedges with the depth of 0.6 and 1.0 dam height are 3.4 and 4.1 cm, respectively. While these values are higher than estimates from other methods, they are within acceptable limits.

## References

1. Mononobe N, Takata A, Matsumura M, (1936). Seismic stability of the earth dam. Proc. 2nd Congress on Large Dams, Washington DC, (4), 1435-
2. Terzaghi K, (1950). Mechanisms of Landslides. In Application of Geology to Engineering Practice, (S. Paige, ed.), pp: 83-125, Geological Society of America, New York, NY, USA.
3. Newmark N.M., (1965). Effects of earthquakes on dams and embankments. *Geotechnique*,15(2)139-
4. Goodman R.E., Seed H.B., (1966). Earthquake-induced displacements in sand embankments. *Journal of the Soil Mechanics and Foundations Division* 90(SM2), 125-
5. Seed H.B., (1966). A Method for Earthquake Resistant Design of Earth Dams. *Journal of the Soil Mechanics and Foundations Division*. ASCE, 92(1),13–
6. Ambraseys N.N., Sarma S.K., (1967). The Response of Earth Dams to Strong Earthquakes. *Geotechnique*, 7, 181-
7. Sarma S.K., (1973). Stability analysis of embankments and slopes. *Geotechnique*, 23 (3):423-
8. Sarma S.K., Bhave M.V., (1974). Critical acceleration versus static factor of safety in stability analysis of earth dams and embankments. *Geotechnique*, 24(4), 661-
9. Sarma S.K., (1975). Seismic stability of earth dams and embankments. *Geotechnique*, 25 (4): 743-
10. Makdisi F.I., Seed H.B., (1978). Simplified procedure for estimating dam and embankment earthquake-induced deformations. *J. Geotech. Engrg., ASCE*, 104, GT7, 849-
11. Seed H.B., (1980). Lessons from the performance of earth dams during earthquakes, *Design of Dams to Resist Earthquake*, ICE, London, 1980, 251-
12. Paskalov T.A., (1984). Permanent displacement estimation on embankment dams due to earthquake excitations. In proceedings of the Eighth World Conference on Earthquake Engineering, July 21-28, 1984, San Francisco, California, U.S.A. 7(D) 327-
13. Paskalov T.A., (1985). Earthquake induced deformations on earth-fill dams and rock-fill dams. *International Journal of Soil Dynamics and Earthquake Engineering*, 4 (1) 35–
14. Hynes-Griffin M.E., Franklin A.G., (1984). Rationalizing the seismic coefficient method. Miscellaneous Paper. GL-84-Vicksburg, Miss, USA: US Army Corps of Engineers Waterways Experiment Station.

15. Finn W.D.L., Yogendrakumar M, Yosida N, Yoshida H, (1986). Tara-3: A Program for Nonlinear Static and Dynamic Effective Stress Analysis. Soil Dynamics Group, University of British Columbia, Vancouver, B.C., Canada.
16. Daghigh Y, (1993). Numerical simulation of Dynamics Behavior of and Earth Dam During seismic loading. Thesis presented to Delf University of Technology Netherland in partial fulfillment of the requirement for the degree of Doctor in Technical sciences.
17. Cai Z, Bathurst RJ, (1995). Deterministic sliding block methods for estimating seismic displacements of earth structures. *Soil Dynamics and Earthquake Engineering*, 15 (4) 255–
18. Matsumoto N, (2002). Evaluation of permanent displacement in seismic analysis of fill dams. In Proc third US-Japan workshop on advanced research on earthquake engineering for dams, San Diego, 22-23 June.
19. Day R.W., (2002). *Geotechnical earthquake engineering handbook*. McGraw-Hill.
20. Swaisgood J.R., (2003). Embankment dam deformations caused by earthquakes. 7th Pacific conference on earthquake engineering, 13-15 February, University of Canterbury Christchurch, New Zealand, paper
21. Wang Z.L., Makdisi F.I., Egan J, (2006). Practical applications of a nonlinear approach to analysis of earthquake-induced liquefaction and deformation of earth structures. *Soil Dynamics and Earthquake Engineering*, 26(4), 231–
22. Han Y, Hart R, (2006). Application of a simple hysteretic damping formulation in dynamic continuum simulations. Proceedings of the fourth international FLAC symposium on numerical modeling in geomechanics, Madrid, Spain. Paper No. 04-R. Hart and P. Varona, Eds.
23. Bray JD, Travasarou T, (2007). Simplified procedure for estimating earthquake-induced deviatoric slope displacements. *J Geotech Geoenviron Eng*, 133 (4) 381–
24. Sica S, Pagano L, (2009). Performance-based analysis of earth dams: Procedures and application to a sample case. *Soils and Foundations*, 49 (6) 921-
25. Rampello S, Cascone E, Grosso N, (2009). Evaluation of the seismic response of a homogeneous earth dam. *Soil Dynamics and Earthquake Engineering*, 29 (5) 782–
26. Jinto H, Davidson R, (2010). Earthquake –induced Displacements of Earth Dams and Embankments. *Australian Geomechanics Journal*, 45 (3) 65-
27. Jibson RW, (2011). Methods for assessing the stability of slopes during earthquakes—A retrospective. *Engineering Geology*, 122 (1-2) 43-
28. Hsieh SU, Lee CT, (2011). Empirical estimation of the Newmark displacement from the Arias intensity and critical acceleration. *Engineering Geology*, 122 (1-2) 34–
29. Davoodi, M., Honardoust, H., Jafari, K. (2013). Study the dynamic behaviour of high and short embankment dams under near-source and far-source earthquakes. Proceeding of 7th NCCE, Zahedan, I. R. Iran.
30. Dong WX, Xu WJ, Yu YZ, Lv H, (2013). Numerical analysis of earthquake response of an ultra-high earth-rockfill dam. *Natural Hazards and Earth System Sciences*, 1 (12) 2319–

31. Bandini V, Biondi G, Cascone E, Rampello S, (2015). A GLE-based model for seismic displacement analysis of slopes including strength degradation and geometry rearrangement. *Soil Dynamics and Earthquake Engineering*, 71 128–
32. Park DS, Kutter BL, (2015). Static and seismic stability of sensitive clay slopes. *Soil Dynamics and Earthquake Engineering*, 79 118–
33. Bray JD, Macedo J, Travasarou T, (2017). Simplified Procedure for Estimating Seismic Slope displacements for subduction zone earthquakes. *J. Geotech. Geoenviron. Eng.*, 144 (3).
34. Ghahreman-Nejad, B., Kan, M. E. (2017). Seismic deformation analysis of embankment dams: A comparison between simplified and non-linear numerical methods. *Proceedings of the 19th International Conference on Soil mechanics and Geotechnical Engineering*, Seoul, Korea.
35. Chen H, Liu D, (2019). Stochastic finite element analysis of rockfill dam considering spatial variability of dam material porosity. *Engineering Computations*, 36 (9) 2929–
36. Rollo F, Rampello S, (2021). Probabilistic assessment of seismic induced slope displacements: an application in Italy. *Bulletin of Earthquake Engineering*, 19, pp:4261–
37. Mazaheri AR, Rozbahani MZ, Beiranvand B, (2020). Quasi-Static and Dynamic Analysis of Vertical and Horizontal Displacements in Earth Dams (Case Study: Azadi Earth Dam). *J. Civil Eng. Mater .App.*, 4 (4) 223–
38. Cho Y, Rathje E M, (2022). Generic predictive model of earthquake-induced slope displacements derived from finite-element analysis. *J. Geotech. Geoenviron*, 148 (4) p:
39. Hwang YW, Rathje EM, (2023). Insights into seismic slope deformation patterns using finite element analysis. *Soil Dynamics and Earthquake Engineering*, 164, p:
40. Zhang, C.Y., Wu, Q., Li, D.Q., and Du, W. (2024). Estimating sliding displacement of slopes induced by earthquake sequences based on the finite element method. *IOP Conf. Series: Earth and Environmental Science*, GeoShanghai 2024 – Volume 1334 012038.
41. Sarma, S. K. Response and stability of earth dams during strong earthquakes. Misc. paper GL-79-13. Geotechnical Laboratory, U.S. Army Engineer Waterways Experiment Station, P.O. Box, 631, Vicksburg, Miss. 39180.
42. Geo-Slope International, Ltd. Geostudio, User manual, Calgary, Alberta, Canada, 1991-2008.
43. Liu C, Macedo J, (2022). Machine learning-based models for estimating seismically-induced slope displacements in subduction earthquake zones. *Soil Dynamics and Earthquake Engineering*, 160, p.
44. Le PH, Nishimura SI, Nishiyama T, Fang C, Nguyen TC, (2022). Seismic Deformation of Earth Dams: A State-of-the-art Review. *Reviews in Agricultural Science*, 10, pp:138–
45. Wang MX, Li DQ, Liu Y, Du WQ, (2022). Probabilistic decoupled approach to estimate seismic rotational displacements of flexible slopes considering depth-dependent soil variability. *Acta Geotechnica*, 17 (4), pp:1551–
46. Bassal PC, Oathes TJ, (2024). Sliding Mass Period for Seismic Displacements of Spatially Variable Slopes. In *Geo-Congress 2024*, pp. 351–

47. Rathje EM, Bray JD, (2000). Nonlinear coupled seismic sliding analysis of earth structures. *Journal of Geotechnical and Geoenvironmental Engineering*, 126, pp: 1002-
48. Meehan CL, Vahedifard F, (2013). Evaluation of simplified methods for predicting earthquake-induced slope displacements in earth dams and embankments. *Engineering Geology*, 152 (1) 180–
49. Ghahreman-Nejad, B., Taiebat, H. A., Noske, C., and Murphy, D.
50. Seismic response and dynamic deformation analysis of SarCheshmeh tailings dam. *Proceedings of the 2nd International FLAC/DEM Symposium in Numerical Modeling*. Melbourne, Australia: Itasca.



© 2024 by the authors. Licensee SCU, Ahvaz, Iran. This article is an open access article distributed under the terms and conditions of the Creative Commons Attribution 4.0 International (CC BY 4.0 license) (<http://creativecommons.org/licenses/by/4.0/>).

